Journal of Nuclear Materials 390–391 (2009) 80–83

Contents lists available at ScienceDirect

Journal of Nuclear Materials

journal homepage: www.elsevier.com/locate/jnucmat

Appearance of hot spots due to deposits in the JET MKII-HD outer divertor

G.J. van Rooij [a,b,*], S. Brezinsek [a,c], J.P. Coad [a,d], W. Fundamenski [a,d], V. Philipps [a,c], G. Arnoux [a,d], M.F. Stamp [a,d], JET EFDA contributors [a,1]

[a] JET-EFDA, Culham Science Centre, OX14 3DB, Abingdon, UK
[b] FOM Institute for Plasma Physics Rijnhuizen, Association EURATOM-FOM, Trilateral Euregio Cluster, Edisonbaan 14, 3439 MN, Nieuwegein, The Netherlands
[c] Institut für Energieforschung-Plasmaphysik, Forschungszentrum Jülich, Association EURATOM-FZJ, Trilateral Euregio Cluster, Jülich, Germany
[d] EURATOM-UKAEA Fusion Association, Culham Science Centre, OX14 3DB, Abingdon, OXON, UK

ARTICLE INFO

PACS:
52.70.Kz
52.40.Hf
52.55.Fa
33.20.Kf

ABSTRACT

Deposited layers in the JET MKII-HD outer divertor have been investigated on the basis of their transient heating. The Planck radiation in the 400–600 nm wavelength range and IR thermography data were analyzed to correlate the appearance of the layers with plasma conditions. Both methods yielded significantly different surface temperatures: typically >2000 K for the visible light spectroscopy and down to 800 K for the thermography. This is explained by the existence of high temperature emission areas as small as 1–2 mm^2. Analysis of the reoccurrence of hot spots in the outer divertor throughout the 2006 campaigns indicated that the formation is determined by the combination of the outer strike point location and the plasma stored energy. The observations did not indicate any changes in thermal properties nor cyclic formation and disintegration of the layers, i.e. it was stable and so-called hard layers.

1. Introduction

Carbon is widely used in present-day fusion experiments and is proposed as wall material for the high power regions in the ITER divertor. However, carbon erosion and transport leads to co-deposition of tritium in deposited layers. Understanding of the formation and migration due to re-erosion and re-deposition of these layers is the starting point for predicting tritium retention due to plasma–wall interaction in these regions. In this contribution, we analyze the behavior of deposits in the JET outer divertor during the 2006 campaigns.

In all divertor configurations in JET, asymmetric deposition of carbon has been observed. Thick flaking deposits were found in the inner divertor close to the pump duct entrance and only little in the outer divertor [1]. This is explained by material eroded predominantly in the main chamber being transported by flows through the SOL (scrape-of-layer) to the inner divertor. The outer divertor seems to be a more closed system in which a local balance between erosion and deposition determines the net material deposition.

In the past, only few cases have been reported in which carbon deposition on the horizontal target of the outer divertor (MKIISRP) was observed [3,5]. The observations were based on the appearance of hot spots attributed to the heating of thin surface films with poor thermal contact to the divertor CFC tile [6]. Usually, this is explained by carbon erosion at the lower vertical target plate and line-of-sight transport to the horizontal target. In this contribution we follow the same approach to identify layers in the JET MKII-HD outer divertor. The pulse history for the cases found is investigated to obtain insight in the conditions that led to the formation of the layers and their stability with respect to disintegration and thermal conductivity. Two approaches are used to detect excursions in surface temperature: IR thermography in the 4.2–4.4 μm wavelength range and analysis of black body radiation in the 0.4–0.6 μm range. The results of both techniques are compared to draw conclusions on the nature of the deposits.

2. Diagnostics and methods

Following the approach described by Stamp et al. [3], we used the central physics file (CPF) database to search for pulses in which the outer target exhibited hot spots. The radiation collected within the range 523–524 nm (this wavelength is used to determine Z-effective from Bremsstrahlung) along a wide angle vertical line-of-sight (l-o-s) that views the outer divertor (see Fig. 1 and [2]) and a horizontal one were compared throughout the 2006 campaigns. If hot surfaces are present in the divertor l-o-s, also Planck radiation will contribute to the signal. At JET, 523.5 nm Planck

* Corresponding author. Address: FOM Institute for Plasma Physics Rijnhuizen, Association EURATOM-FOM, Trilateral Euregio Cluster, Edisonbaan 14, 3439 MN, Nieuwegein, The Netherlands.
E-mail address: rooij@rijnhuizen.nl (G.J. van Rooij).
URL: http://www.rijnhuizen.nl (G.J. van Rooij).
[1] See Appendix of M.L. Watkins et al. Proc. 21st Int. Conf. Chengdu, 2006, IAEA (2006).

0022-3115/$ - see front matter © 2009 G.J. van Rooij. Published by Elsevier B.V. All rights reserved.
doi:10.1016/j.jnucmat.2009.01.083

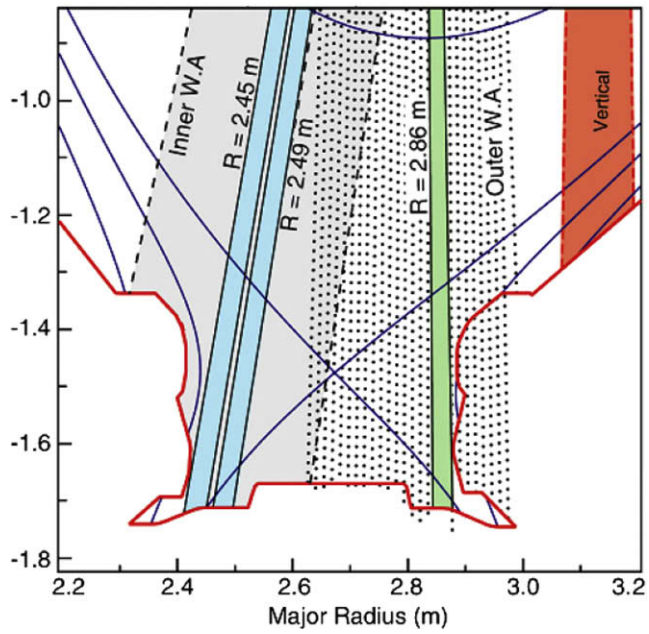

Fig. 1. Schematic of the lines of sight viewing the outer divertor. A wide angle l-o-s covered the entire outer divertor and was used to select pulses with the hot spots in this region. The 33 mm diameter high resolution vertical l-o-s crossed the horizontal target at major radius $R = 2.87$ m and was used to analyze the hot spot temperature and emissivity in the 400–600 nm wavelength range.

radiation exceeds the Bremsstrahlung level if the surface temperature is >1900 K. Short-lived hot spots (e.g. <1 ms due to ELMs) are only detected at even higher temperatures. Given the 50 ms exposure time of the detectors, 1 ms hot spots of >2600 K will be detectable.

A second l-o-s of 33 mm diameter that intersects the outer vertical divertor target at 2.873 m (see Fig. 1) was analyzed with the JET visible survey spectrometer spectrometer KS3A. KS3A is a custom built CCD spectrometer utilising SLR camera optics ($f = 135$ mm collimating lens, $f = 85$ mm focussing lens) and a 1200 l/mm, 120 mm × 120 mm ruled diffraction grating with a 1024 × 1024 pixel frame-transfer CCD camera. The wavelength coverage is 420–620 nm with an instrumental FWHM of 2.8 pixels. Spectra are recorded with a 50 ms exposure time at 20 Hz. These spectra are used to determine hot spot temperatures from the black body radiation.

The JET wide angle IR thermography was used to determine the surface temperatures in the divertor [4]. The system was operating with a 4.2–4.4 μm band filter at 50 Hz. Typical spatial resolution of the system is ~6 mm. The maximum temperature was for these measurements ~1200 °C.

3. Results

3.1. Location of the hot spots

Table 1 lists all 2006 pulses that were selected on the basis of strong Planck radiation around 523 nm from the outer vertical target of the MKII-HD divertor. These data show that the strike point was always close to the pumping duct in the outer divertor corner at a major radius $R > 2.87$ m. In addition, the diamagnetic energy was always larger than 3 MJ. Detailed analysis of these pulses and those in adjacent sessions indicated that these are the main requirements for the occurrence of hot spots in the outer divertor. In fact, similar discharges with the strike point at a major radius less than 1 cm shorter than 2.87 m did not lead to significant Planck radiation. A drop in the diamagnetic energy below ~1 MJ caused existing

Table 1
All 2006 pulses that exhibited strong Planck radiation from the outer vertical divertor target at 523 nm. Listed are the time T, the position of the outer strike point RSOL, the ratio between the horizontal and vertical intensity Hor/Ver, the absolute intensity recorded along the horizontal wide angle l-o-s $I(532)$, and the diamagnetic energy WDIA at the moment of maximum Planck radiation.

Pulse	T (s)	RSOL (m)	Hor/Ver	$I(523)$ (10^{23} ph/s/cm^2/sr/nm)	WDIA (MJ)
65588	53.1362	2.877018	75.91794	2.96E+13	2.50E+06
65596	53.1362	2.874218	44.10788	2.27E+13	2.70E+06
66147	57.8786	2.905081	58.57692	2.53E+13	5.50E+06
66148	59.3682	2.919744	44.05071	2.15E+13	3.50E+06
66456	55.8722	2.884296	45.05529	1.54E+13	5.00E+06
66457	55.8722	2.884731	45.69799	9.02E+12	5.00E+06
66458	55.8722	2.88471	40.17187	7.42E+12	5.00E+06
66470	55.629	2.882135	54.74974	1.26E+13	5.00E+06
66779	54.869	2.890318	70.99383	1.37E+13	No data
66780	54.869	2.889757	55.34927	9.41E+12	No data
67952	57.6354	2.925987	62.98306	3.70E+13	No data
67954	57.6354	2.927376	51.27206	2.59E+13	No data
67955	57.6354	2.925907	62.8263	3.11E+13	No data
68380	48.3938	2.909559	54.61843	2.28E+13	4.00E+06
68381	48.8802	2.912979	65.59094	2.62E+13	4.00E+06
68382	48.8802	2.919033	80.89357	3.57E+13	4.00E+06
68383	49.3666	2.910435	115.0172	3.94E+13	4.00E+06
68384	53.8658	2.913273	80.7856	4.20E+13	4.00E+06
68386	49.3666	2.910477	146.7405	5.01E+13	4.00E+06
68387	49.3666	2.906923	103.1524	3.26E+13	4.00E+06
68393	53.8658	2.917456	190.3552	9.87E+13	5.00E+06
68394	52.3762	2.919952	243.1213	1.02E+14	5.00E+06
68554	61.1162	2.904701	40.69737	4.08E+13	4.00E+06

hot spots to extinct. It is noted in this context that the listed strike point locations are based on EFIT magnetic reconstructions. The real outer strike point location may be up to 2 cm shifted, depending on the magnetic pressure and ELMs. This was observed e.g. early in discharge 68 554 (at $t = 15.7$ s) were due to an increasing a hot spot was formed at an apparently constant strike point position.

Pulse #69554 was a unique experiment for visualization of the location of the deposited layer causing the hot spot. It contained a slow sweep of the outer strike point over the region $2.86 < R < 2.92$ during the heating phase. Fig. 2 shows the details of this pulse. Both the contribution from black body radiation to the Bremsstrahlung signal and the maximum surface temperature of the horizontal outer divertor target measured with IR thermography contain the signature of a hot spot when the outer strike point is beyond 2.885 m major radius. The Bremsstrahlung l-o-s does not detect the hot layer when the strike point is beyond 2.900 m. This is caused by the limited width of the l-o-s, which ends at this position. The tangential IR view covers the entire target and detects the hot layer up to ~2.915 m. At this position, the heating phase was ended (see WDIA) and the power fluxes at the strike point become too small to heat the layer.

The IR signal contains also spikes on the temperature measurement when the strike point is still away from the layer. These excursions coincide with the occurrence of ELMs. We interpret this as the result of a slight movement of the strike point during the ELM. The visible signal is observed to be less sensitive to the heating during ELMs due to the larger integration time.

3.2. Temperature measurements

The evolution of the peak temperature measured by IR thermography on the outer divertor target and the temperatures that were deduced by fitting the background in the visible spectrum with the Planck curve for black body radiation for the preceding pulse (#68553) are compared in Fig. 3. The heating phase of pulse #68553 was shorter (between $t = 12$–19 s) than in the slow sweep pulse #68554 and the strike point was moved between $R = 2{:}86$–2:89 m, so only just reaching the border of the layer. As a result,

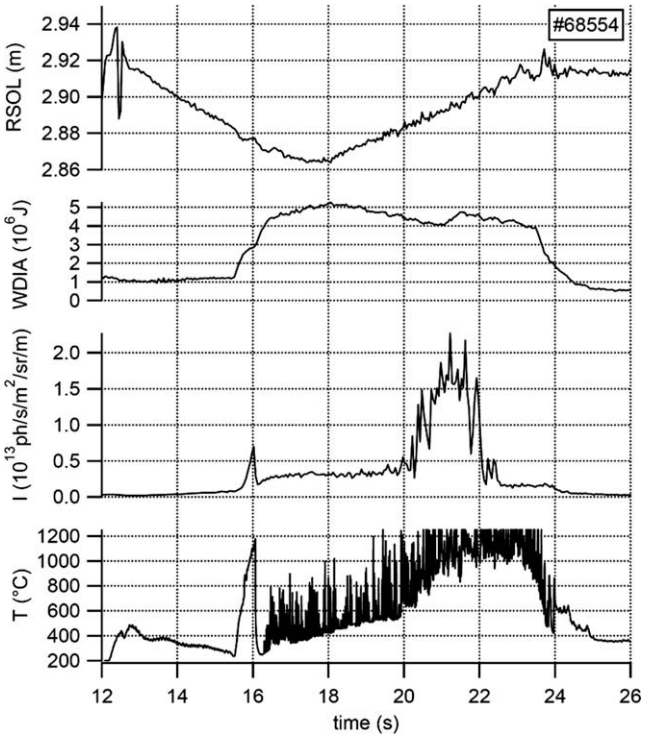

Fig. 2. Pulse #68554 contained a sweep of the outer strike point over the layer in the outer divertor. (a) shows the position of the outer strike point, (b) the diamagnetic energy, (c) the signal in the vertical l-o-s monitoring 523 nm Bremsstrahlung, and (d) the maximum temperature measured on the outer divertor horizontal tile by IR thermography (which saturated above 1200 K).

the temperature excursions in the IR are much more moderate compared to pulse # 68554. The temperatures determined from the spectrum in the visible are up to 1000 °C higher, in particular when the hot spot occurs for the first time at t = 15:5 s. At the end of the sweep, at $t \sim$ 18:8 s, the surface temperature exceeds the dynamic range of the IR system and it is difficult to judge any (dis-)agreements.

In order to determine the origin of the observed disagreement between the two temperature determinations, the black body

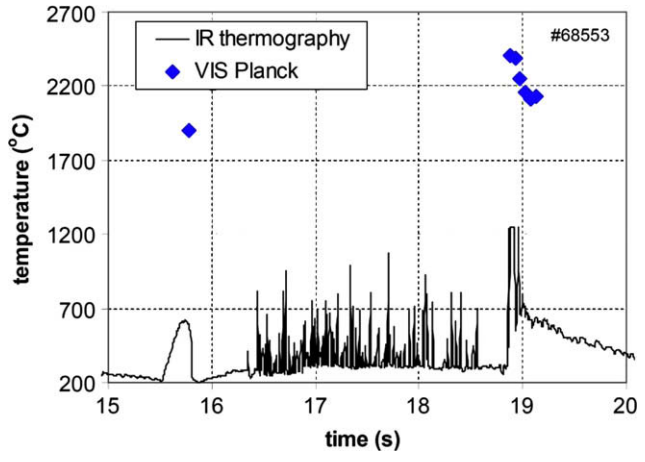

Fig. 3. Comparison of the maximum temperature at the horizontal outer divertor target measured with IR thermography and the temperature deduced from the black body radiation in the 400–600 nm wavelength range (KS3A, track 6) for pulse #68553. The black body contribution in the visible was too low to allow fitting with a Planck curve where no data is plotted. At t = 18.8 s, the dynamic range of the IR system is exceeded.

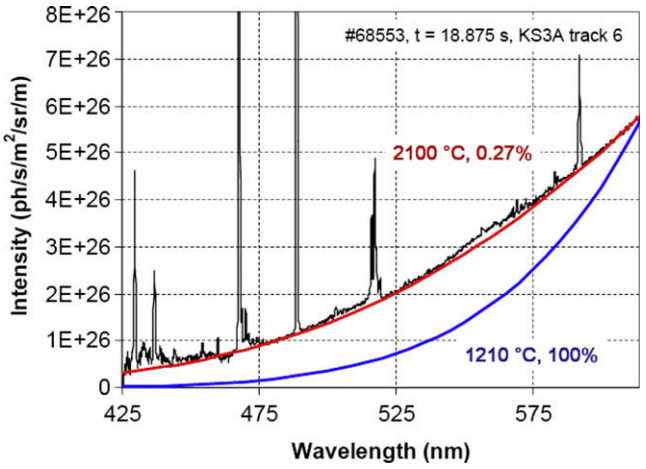

Fig. 4. Spectrum exhibiting black body radiation (pulse #68553, t = 18:875 s, KS3A track 6). The base line is fitted with Planck curves. Assuming 100% emission area and fitting the emission at 615 nm yields 1210 °C but underestimates the black body radiation at lower wavelengths. With the effective emission area as a free parameter, the temperature is fitted to 2100 °C and the area to 0.27%.

radiation is inspected in detail in Fig. 4. It is seen that the emitted power and the spectral shape do not correspond in temperature. If a 100% emission area (and unity emissivity) is assumed, the radiated power at 600 nm would correspond to a temperature of 1200 °C. Fitting the Planck curve to the entire spectral baseline, the surface temperature should have been 2100 °C, but the radiated power at 600 nm would be a factor of 370 too low. This implies a limited effective emission area of 1/370 = 0.27%. A granular nature of the hot spot would explain such a small effective area, in consistence with [3].

These observations lead to the picture that the analysis in the visible spectrum is more sensitive to small features at high temperatures whereas the IR measurements represent some kind of average over the entire surface. The question remains whether both measurements represent the same physics. Starting from the results in the visible, an effective emission area of 0.25% for the 33 mm diameter l-o-s corresponds to a hot structure of 2 mm^2. The IR spatial resolution was 6 × 6 mm, thus here the hot feature constitutes 6% of a spatial element. If the overall temperature of the layer was 1000 °C (as for pulse #68554, t = 21–23 s), the contribution of this small hot spot would have been 20%. This contribution would have increased the outcome of the IR measurement by 100 °C. For a cold background of 200 °C (as for pulse #68553, t = 16 s), the hot feature would dominate the IR measurement. This would lead to a temperature reading of 560 °C, which is in fact very close to the experimental values in Fig. 3. Here, the temperature excursion in the IR measurement at t = 15:7 s is indeed matching the radiated power from the high temperature feature detected in the visible.

3.3. Stability of the high temperature surface component

In order to assess the stability of the high temperature features measured in the visible spectrum, we return to the data of pulse #68553 in Fig. 3. It is seen that the temperature determined from the visible spectrum decays from 2130 °C to 1860 °C within 0.25 s. Not only the temperature decreased, but also the effective emission area: from 0.25% to 0.10% (data not shown). This is indicative of a physical removal of the feature, e.g. removal of so-called soft deposits. Evaluation of the pulse sequence #68553–#68555 indicates that this is not the case.

After the slow sweep in pulse #68554, which induced even slightly higher temperatures than the previous one and was

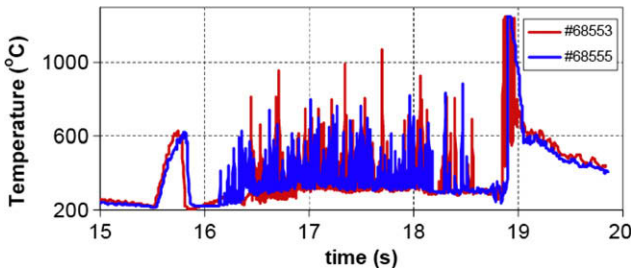

Fig. 5. Peak temperature in the outer divertor determined with IR thermography in pulse #68553 and #68555, which were identical. It demonstrates that all hot features remain essentially unchanged, which shows that these are stable.

expected to remove all soft features, the first pulse was repeated. In Fig. 5 the peak temperature measured with IR thermography of pulses #68553 and #68555 are compared. This demonstrates that the temperature excursions are essentially the same, which shows that the hot features are stable. Evaluation of the visible spectrum confirmed this view.

4. Summary and conclusions

We have demonstrated that the absolutely calibrated survey spectrometer (423–614 nm) and the IR thermography provide complimentary information on the surface temperature and temperature homogeneity. The former is most sensitive to temperatures above ~2000 °C at emission areas down to 1–2 mm^2, whereas the latter yields values averaged over ~36 mm^2.

Analysis of all 2006 pulses exhibiting hot spots learned that there exists a stable deposited layer on the vertical outer divertor target at a major radius >2.885 m. Also the granular features exhibiting temperature excursions up to 2200 °C were found to be stable.

It is evident that power balance calculations on basis of IR thermography temperatures are inuenced by the existence of small high temperature features on the surface. It should be possible to combine both diagnostics so that the temperature and emission area information from the visible spectrum are used to correct the temperatures measured by IR thermography.

Acknowledgements

This work has been performed under the European Fusion Development Agreement. The views and opinions expressed herein do not necessarily reflect those of the European Commission. It was also supported by the FOM-Institute for Plasma Physics Rijnhuizen, partner in the Trilateral Euregio Cluster, in the frame of the Contract of Associated Laboratory, with financial support from NWO.

References

[1] J.P. Coad, J. Likonen, M. Rubel, E. Vainonen-Ahlgren, D.E. Hole, T. Sajavaara, T. Renvall, G.F. Matthews, et al., Nucl. Fus. 46 (2006) 350.
[2] M.F. Stamp et al., Phys. Scr. T91 (2001) 13.
[3] M.F. Stamp, P. Andrew, S. Brezinsek, A. Huber, et al., J. Nucl. Mater. 337–339 (2005) 1038.
[4] E. Gauthier, P. Andrew, G. Arnoux, Y. Corre, H. Roche, et al., J. Nucl. Mater. 363–365 (2007) 1026.
[5] J.P. Coad, P. Andrew, D.E. Hole, et al., J. Nucl. Mater. 313–316 (2003) 419.
[6] P. Andrew, J.P. Coad, T. Eich, et al., J. Nucl. Mater. 313–316 (2003) 135.